Estimating Climate Change-based Soil Loss Using Erosion Models and UAV Imagery in the Metsovo Mountain Region

Loukas-Moysis Misthos [1], Lefkothea Papada [2], George Panagiotopoulos [3], Nikos Gakis [4], Dimitris Kaliampakos [5]

[1] National Technical University of Athens, School of Mining and Metallurgical Engineering, Zographou, Greece, (lmisthos@central.ntua.gr)
[2] National Technical University of Athens, Metsovion Interdisciplinary Research Center, Metsovo, Greece, (lefkipap@metal.ntua.gr)
[3] National Technical University of Athens, Metsovion Interdisciplinary Research Center, Metsovo, Greece, (g.panag@metal.ntua.gr)
[4] National Technical University of Athens, School of Mining and Metallurgical Engineering, Zographou, Greece, (ngakis@facets.gr)
[5] National Technical University of Athens, School of Mining and Metallurgical Engineering, Zographou, Greece, (dkal@central.ntua.gr)

Key words: *accelerated water erosion*; *soil loss estimation*; *climate change*; *UAV imagery*; *geospatial modelling*

ABSTRACT

Soil erosion is a natural process involving soil loss rates of about 2 t ha^{-1} $year^{-1}$. This process can be heavily intensified due to human activity, inducing losses of up to 100 t ha^{-1} $year^{-1}$, further leading to significant land cover alteration and soil productivity decrease. Climate change is a human-induced agent that affects several factors underlying soil erosion in various ways. In mountain areas, climate change may be significantly detrimental to the landscape and soil productivity, especially for the upper convex hillslope parts (summits, shoulders etc.), where soil displacement is not frequently counterbalanced by soil formation. In this paper, a methodology for estimating and mapping soil loss by water erosion in a mountainous region (Metsovo, Greece) is developed. To this end, an effective erosion model (RUSLE) is utilized by combining and fine-tuning data from climate models, geospatial data, and UAV imagery: the climate models are downscaled providing input data; the UAV, equipped with a multispectral sensor, supports precise land cover classification, DEM generation and the computation of suitable indices. The results show that both the enhanced land classification scheme derived from the UAV imagery, and the future scenarios regarding climate and rainfall erosivity change affect the estimated soil loss rates. The aggravated soil loss rates are meant to deform more seriously the more elevated and rugged parts of the landscape, while the subsequent land degradation poses environmental and socio-economic concerns for the mountainous but productive and active region of Metsovo, under the influence of climate change.

I. Introduction

A. *Soil Loss and Erosion Models*

One of the major consequences of water erosion is soil loss. Soil loss rates of about 2 t ha^{-1} $year^{-1}$ occur due to natural erosional processes (Nearing *et al.*, 2017). This type of erosion (geological) can be significantly aggravated by human intervention, inducing losses of up to 100 t ha^{-1} $year^{-1}$ (Julien, 2010), further leading to significant terrain deformation, land degradation, soil productivity decrease and overall environmental quality degradation (Pimentel, 2006; Lal, 2014).

Aside from the significance of understanding the underlying rainfall erosion processes (e.g. Wainwright *et. al.,* 2003), identifying the areas susceptible to erosion and quantitatively estimating the soil loss is crucial towards the development of proper soil protection practices (Shi *et al.,* 2004). Erosion models support these two – theoretical and practical – dimensions and have led to the systematic investigation of the interplaying factors affecting the processes. In essence, the climate-topography-soil-vegetation 'nexus' summarizes the generic erosion process, while soil loss is one of the main measured features, associated with the quantitative description of the erosion consequences.

In a recent review paper (Karydas *et al.*, 2014), among over 80 erosion models, the (R)USLE ((Revised) Universal Soil Loss Equation) family models are shown to be adequate approximations for modelling the soil loss feature of the overall water erosion process. Such models and, especially the RUSLE ones, are GIS-based models employing geospatial analyses that are not limited to the simple map algebra or overlaying functions (for raster and vector geo-datasets, respectively). Contrariwise, they employ *Pathway* (PW) type methodologies, in the sense that they incorporate topological relations (e.g. neighborhood or proximity),

while their outputs are computed based on stepwise techniques (e.g. flow accumulation, network analysis). Overall, they are suitable for "field- to hillslope-scale, temporally averaged assessments of soil loss" (Karydas *et al.*, 2014: 242).

The fundamental equation underlying the RUSLE GIS-based models is the following (Renard *et al.*, 1997; Panagos *et al.*, 2015a):

$$E_A = R * K * LS * C * P \quad (1)$$

where E_A: annual average soil loss (t ha^{-1} year^{-1})

R: rainfall erosivity/ erodibility factor (MJ mm ha^{-1} h^{-1} year^{-1})

K: soil erodibility factor (t ha h ha^{-1} year^{-1} MJ^{-1} mm^{-1})

LS: slope length and slope steepness (topographic) factor (dimensionless)

C: cover-management factor (dimensionless)

P: support practices factor (dimensionless)

Yet, the calculation of the annual average soil loss and the attribution of spatial reference to the corresponding results (i.e. production of soil loss maps) requires processing and adjustment of the multifarious (geospatial) input data (climatic, topographic etc.) and implementation of appropriate geospatial analyses. Towards this end, the 'incorporation' of the RUSLE in GIS environments – an already entrenched approach (e.g. Prasannakumar *et al.* 2012; Gupta and Kumar, 2017) – needs to be applied by means of an explicit geo-spatial approach and by making use of parameterizable input data. Climate change, potentially aggravating the accelerated erosion or soil loss (Li and Fang, 2016), is considered a modifier of some of the five factors of the RUSLE model (Gupta and Kumar, 2017). Its effect, particularly in mountain regions, is described in the subsequent section.

B. *Climate Change and Soil Loss in Mountain Regions*

Soil loss due to water erosion constitutes a major problem of soil degradation and terrain deformation in mountain regions of Greece. It depends both on climate conditions (mainly atmospheric precipitation) and on terrain and vegetation features.

Regarding the part of landscape, mountain regions are more susceptible to soil erosion, mainly due to (a) their intense relief with steep slopes, (b) the presence of shallow soils (lithosols) and a fairly high percentage of impermeable rocks, (c) the frequent forest fires and (d) the poor soil management practices / unreasonable use of natural resources, i.e. land clearing and cultivation of highly sloping soils, unreasonable logging, overgrazing, etc. As far as climate conditions are concerned, climate change is expected to affect spatial expansion, frequency and magnitude (intensity) of soil erosion in a variety of ways (Pruski and Nearing, 2002; Mullan *et al.*, 2012). These impacts may be direct and associated with variations in the amount of precipitation (Nearing *et al.,* 2004; Bangash *et al.,* 2013), the intensity of precipitation (Zhang, 2012), or its spatio-temporal allocation patterns (Maeda *et al.,* 2010; Li and Fang, 2016). However, the impacts may be indirect and related to the new climate regime, mainly through temperature rise (Mullan *et al.,* 2012; Li and Fang, 2016), a fact reflected in vegetation changes, as well as in soil moisture (Nearing *et al.,* 2004; Li and Fang, 2016). The most 'remote' indirect impacts include cultivation practices adopted (e.g. changes in sowing and harvesting periods or crop varieties), as responses to precipitation changes (Nunes and Nearing, 2011; Parajuli *et al.,* 2016).

Beyond temperature and precipitation, variables such as relative humidity, clouds, wind, etc. are expected to change in the general context of climate change (Flannigan *et al.,* 2006), modifying, in this way, extreme events, such as increased periods of heat-wave conditions, increase of the frequency and intensity of storms/floods/prolonged droughts during the summer period and increase of lighting fires (Mearns *et al.,* 1989; Solomon and Leemans, 1997). These phenomena, as well as other crucial factors in mountain regions such as forest fires, aggravate soil erosion rates (Inbar *et al.,* 1998; Kosmas *et al.,* 2006; McNabb and Swanson, 1990; Dieckmann *et al.,* 1992).

Therefore, climate change has a significant impact on soil loss due to water erosion. The quantification of this impact should be included in relevant models, in order to realistically assess annual average soil loss in an integrated way. Towards this end, climate models are utilized.

Global Climate Models (GCMs) are the primary tools used for making projections of the future climate (Flato *et al.*, 2013). Even though GCMs have been developed and improved, they still provide projections of climate variables, such as precipitation and temperature, at a spatial resolution of 100-300 km. This resolution is too coarse to be directly used in local impact studies (Yang *et al.*, 2015; Gupta and Kumar, 2017), especially in mountainous areas which are characterized by complex topography with alternations of vegetation and land cover within a few kilometers (Pepin *et al.*, 2015). Climate projections for Europe derived from dynamic downscaling at grid resolutions of about 12km are available in the database of the EURO-CORDEX initiative (Jacob *et al.*, 2014). However, hydrological models often require rainfall data of higher spatial resolution, thus spatial interpolation techniques such as Nearest Neighbor (NN), Thiessen polygons, Spline and various forms of Kriging and Inverse Distance Weighting (IDW) are applied to further downscale RCM's (Regional Climate Models') rainfall data (Yang *et al.*, 2015). In addition, the direct application of RCMs in many impact modelling studies is hampered by model biases,

therefore bias correction techniques are applied to ensure a better agreement between models and observations (Casanueva *et al.*, 2015).

C. *Aims and Rationale*

Since erosion processes in mountainous areas are associated to great soil losses, this paper aims at the development of a methodology for estimating this loss in a typical mountainous region of Greece, Metsovo, based on the RUSLE model (Renard *et al.*, 1997; Panagos *et al.*, 2015). This methodology utilizes data derived from climatic models and from UAV's multispectral image captures employing geospatial analyses. The introduction of climatic data referring to future dates and refined land cover geospatial data, along with their integration into erosion models, are novel contributions resulting in more fine-tuned and climate change-based soil loss estimations. In essence, in the proposed soil loss model, the R-, C-, LS and P-factors are parameterized and calculated on the basis of future rainfall intensity and different classification schemes according to well-established practices, while K-factor is acquired by pertinent databases (Figure 1).

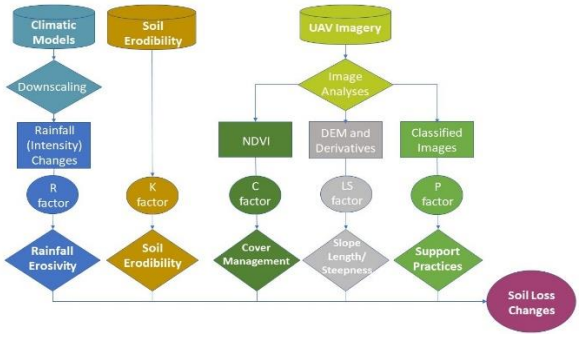

Figure 1. Inputs-outputs for the proposed Climate Change-based Soil Loss Model. R-factor is affected by climate change data, while C-, LS- and P-factors get refined inputs from processed UAV imagery (based on Panagos *et al.*, 2015a - modified)

II. Main Body

A. *Study Area*

The study area, Metsovo, is located in a mountainous region of Greece, called Epirus. More precisely, a 1.3 km^2 area in the wider area of Metsovo town is selected due to its increased water erosion problems.

The area, with a mean elevation exceeding 1000 m and rather steep hillslopes (mean slope > 15°), presents increased rainfall and precipitation (> 1000 mm year^{-1}), while its general land cover is characterized by mixed croplands, natural grasslands and coniferous forests.

B. *Data Collection and Initial Processing*

For the estimation of the annual average soil loss (E_A), the RUSLE model was implemented in a GIS environment. Therefore, the data for each RUSLE factor were collected and processed in order to constitute suitable geospatial input data for the model.

Climatic Data

For the study area, data of precipitation for the period 1961-2000 (historic climate) and the period 2011-2050 (future climate) were obtained from the EURO-CORDEX database, in the form of monthly time series. The data are downscaled simulations of the RACMOE22 regional model driven by EC-EARTH global model for two RCP (Representative Concentration Pathway) scenarios, namely RCP4.5 and RCP8.0, in a spatial resolution of 0.11°. Data of both historical and future period were downscaled at a point level using the Nearest Neighbour method. Downscaled climate data were bias-corrected using daily precipitation data for the period 1961-1990 from the hydrometeorological station of Greek ministry of Environment in Metsovo, available in the database of the research project Hydroscope (Sakellariou *et al.*, 1994).

Soil Data

Soil data were acquired from the European Soil Database v2 Raster Library 1kmx1km (Panagos, 2006; Van et al., 2006) and the cartographic portal of the Institute of Geology and Mineral Exploration (IGME)[1]. The European Soil Database provides data for various soil properties of which the soil erodibility class and soil classification raster layers were used. According to the IGME cartographic portal, the study area lies entirely on top of a sandstone layer, displaying very strong erodibility.

UAV Imagery and Land Cover Data

The area was scanned with an UAV taking multiple multispectral captures with a constant interval, utilizing *PiX4Dcapture* flight technology which provides the user the ability to completely scan a certain area along a grid, the resolution of which is automatically computed based on the UAV's flight altitude. Due to the rugged terrain of the area, the flight altitude ranged approximately between 50 – 300m. The multispectral images were georeferenced and merged together in a seamless mosaic using *AgiSoft PhotoScan*®. By this procedure, a multispectral (1.2MP), 4-band (Green, Red, Red Edge, and Near Infrared (NIR)) image (1m spatial resolution) of the study area was produced. The image was further classified on the basis of an object-oriented, multiresolution procedure, using eCognition® software. The image was initially segmented by making several trials, and then was classified in 6 classes/ land covers using the samples' method. The results of the

[1] Geoportal's website: http://www.igme.gr/geoportal/

produced land cover map were verified by means of *ground truthing*[2].

Topographic Data – DEM

The AgiSoft PhotoScan® software was also employed to generate the DEM (Digital Elevation Model) of the area. DSM (Digital Surface Model) is generated from the software by taking into consideration the complete point dense cloud, while DEM was derived based on ground points only. The classification of the ground points was attained by properly defining certain thresholds regarding surface points' angle and distance. The spatial (x,y) resolution of the generated DEM was 1 m, while its z-information was calibrated using elevation ground control points. DEM's elevation values ranged from 899 m to 1178 m (Figure 2), with mean and standard deviation values of 1008.93 m and 58.87 m, correspondingly.

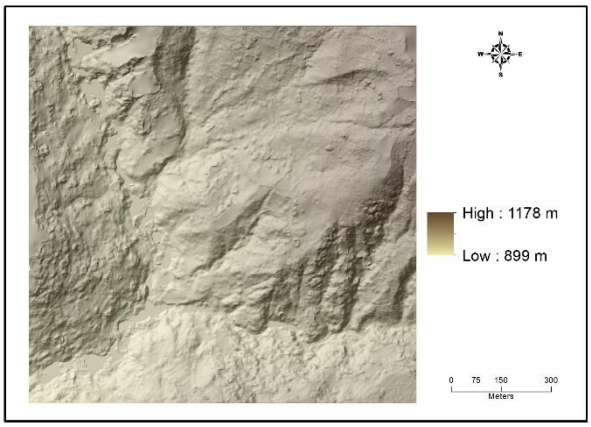

Figure 2. DEM derived from the UAV captures

C. *Methodology - RUSLE Factor Generation*

The methodology utilized refers to the calculation of each of the RUSLE equation factors and the overall implementation of RUSLE, employing raster-based geospatial analyses in a GIS environment. In the following part, the computation of each of the five factors in a GIS environment is described. E_A results from the multiplication of the cell values of each of the five raster intermediate outputs through a map algebra operation.

Rainfall Erosivity (R)

The erosive force of rainfall is commonly expressed by the R-factor of the RUSLE model, which combines the effects of duration, magnitude and intensity of each rainfall event (Panagos *et al.*, 2015c). R-factor is calculated as the product of storm kinetic energy and maximum 30-min intensity (EI30) of each storm event, while its analytical calculation requires sub-hourly precipitation data for a long period over 20 years (Hernando and Romana, 2015). Historical records of these data are usually not available in many regions, including the Mediterranean region (Diodato and Bellocchi, 2010), while the output of climate models does not provide data with sufficient temporal resolution (Shiono *et al.* 2013; Panagos *et al.*, 2017). Therefore, various simplified empirical models have been proposed for estimating R-factor from daily, monthly or annual precipitation data (Yin *et al.*, 2015). For the case of Greece, there are equations for the estimation of monthly R-factor (Panagos *et al.*, 2016) and annual R-factor (Flambouris, 2008), as functions of monthly and annual precipitation, respectively. However, these relationships do not consider the precipitation extremes (e.g. maximum daily precipitation), which are related to rainfall intensity.

Diodato and Bellocchi (2010), analyzing the detailed multi-year datasets from 66 weather stations in the Mediterranean basin, proposed the following simplified equation (Model MedREM) for the calculation of multi-year R-factor in MJ mm ha^{-1} h^{-1} y^{-1} in a location:

$$R = b_o \cdot P \cdot \sqrt{d} \cdot (a + b_1 \cdot L) \quad (2)$$

where *a*, b_o, *and* b_1*:* coefficients with values 2.000, 0.117 and -0.015, respectively

P: annual rainfall (mm y^{-1})

d: annual maximum daily rainfall (mm d^{-1} over a multi-year period)

L: location longitude (º)

According to the validation performed by Diodato and Bellocchi (2010), the MedREM estimates fitted well with the R-factor values calculated from analytical data of 55 stations in the region and, hence, MedREM is recommended for long-term annual erosivity estimations in the Mediterranean.

Annual rainfall and annual maximum daily rainfall for Metsovo were computed from downscaled and bias-corrected daily rainfall data for two periods, namely 2011-2030 (short-term) and 2031-2050 (long-term) and the two RCP scenarios (RCP4.5 and RCP8.5). Average annual and annual maximum daily rainfall over these periods were used as input in the MedREM equation in order to estimate R-factor. The results are presented in Tables 1 and 2 for scenarios RCP4.5 and RCP8.5, respectively. According to the results, the projected rainfall erosivity is expected to increase until 2050 in Metsovo approximately 97 MJ mm ha^{-1} h^{-1} y^{-1} in the RCP4.5 scenario (5,8%) and 366 MJ mm ha^{-1} h^{-1} y^{-1} in the RCP8.5 scenario (21,9%) compared to the current period 2011-2013 due to increase of both annual rainfall and daily maximum rainfall.

[2] Due to the high resolution of the images captured in a relatively low altitude, the photointerpretation of the image enabled the comparison of the classified map with the actual features of the images. However, we had to classify the UAV imagery according to the CLC classes, in order to be able to compare the output classes of the UAV classification with the CLC classification. So, the validation was based on the photointerpretation, restricted by the CLC classification.

Table 1. Climate data and R-factor for RCP4.5 and RCP8.5 scenarios

	RCP4.5		RCP8.5	
Period	2011-2030	2031-2050	2011-2030	2031-2050
P (mm y^{-1})	1210.6	1277.1	1179	1361
d (mm d^{-1})	55.8	64.9	52.8	58.9
R (MJ mm ha^{-1} h^{-1} y^{-1})	1683	1780	1672	2038

Soil Erodibility (K)

Soil erodibility measures the susceptibility of soil particles to detachment and depends on several soil properties such as texture, structure, organic matter content etc. (Gupta and Kumar, 2017). Erodibility values for the study area were retrieved from a high-resolution (500m grid cell) erodibility dataset (Panagos *et al.*, 2014 Metsovo presents very strong erodibility values (0.05 t ha h ha^{-1} MJ^{-1} mm^{-1}), since it is located on a flysch layer where erosion and landslides are common.

Slope length and steepness factor (LS)

The LS factor refers to the combination of the L- and S-factors. It estimates the combined effect of the slope length (L) and the slope steepness (S) of the terrain on the loss of soil. In the present analysis, the LS-factor was computed within a GIS environment, as a function of two DEM derivatives, namely slope steepness (SS) and flow accumulation (FA), according to the following equation proposed by Moore and Burch (1986a; 1986b):

$$LS = \left(FA * \frac{Cell\ Size}{22.13}\right)^{0.4} * \left(\frac{\sin SL}{0.0896}\right)^{1.3} \quad (3)$$

where LS: combined slope length/ steepness factor

FA: the accumulated upslope contributing area for a given cell

Cell Size: the size of the grid cell: 1 m

$\sin SL$: the slope degree value in sin

For this study area, the LS-factor ranges from 0.36 to 45.41, with the vast majority of the study area displaying LS values lower than 4, while LS values higher than 15 occupy a very small percentage of the study area.

Cover Management Factor (C)

Since land cover/ use and related management affect the magnitude of soil loss (Panagos *et al.*, 2015b), C-factor is meant to represent the soil-disturbing uses and activities. It is defined as the ratio of soil loss under the given vegetation cover/ conditions to the loss occurring under continuous bare-soil conditions (Alexandridis *et al.*, 2013). In the present analysis, C-factor is calculated by resorting to remote sensing ratios, as follows (Van der Knijff *et al.*, 1999):

$$C = exp\left(-a * \frac{NDVI}{\beta - NDVI}\right) \quad (4)$$

where $NDVI$: Normalized Difference Vegetation Index – (NIR-RED / (NIR+RED) –, being an indicator of the vegetation vigor

α, β: Parameters determining the shape of the NDVI-C curve. Values of 2 and 1, respectively, have been found to yield reasonable results (Van der Knijff *et al.*, 1999; Prasannakumar *et al.*, 2012)

Using this equation, the values for the C-factor for area under study varied between 0.07 and 1.53. It is worth noticing that this equation adequately approximates C-factor since it has been successfully applied in areas featuring similar climatic, terrain, and land cover conditions (e.g. Prasannakumar *et al.*, 2012) with these of the present study area. The usage of UAV imagery and NDVI enhances C-factor's quality compared to the usage of other sources (outputs in existing databases or from satellite imagery), since it supports more refined and accurate estimations of the factor which are better suited to the characteristics of the specific study area.

Support Practices (P)

P-factor represents the soil loss ratio with a specific support practice to the corresponding soil loss with straight-row tillage up and down the slope (Renard *et al.*, 1997). Of the five RUSLE factors, the values attributed to this factor are the most uncertain (Morgan and Nearing, 2011).

In this study, the values for P-factor were attributed based on the land cover. Two classification schemes were utilized: a CORINE Land Cover (CLC) (2012)[3], and the result of the classification based on the UAV multispectral images. Higher values correspond to areas with no conservation (natural grasslands, built-up, forest), whereas the lowest values were assigned to areas occupied by agriculture, potentially applying strip/ contour cropping (Table 3). It should be noted that the higher resolution of the UAV photogrammetric reconstruction enabled a more detailed and reliable classification of the area. That is why in the case of the UAV classification 6 land cover classes occurred compared to the 4 classes of the CLC.

Table 3. P-factor values and percentage of area for each land cover, under the two classification schemes (CLC 2012 and UAV classifications)

	CLC 2012		UAV	
Land Cover/ Area	P-factor	Area (%)	P-factor	Area (%)
Built-up	0.8	0.50	0.8	3.29
Paved	-	-	0.9	2.59
Agricultural	0.4	63.21	0.4	47.89
Coniferous forest	0.8	4.58	0.8	6.77
Natural grassland	1	31.71	1	29.63
Sparsely vegetated	-	-	0.7	9.83

[3] CEU, Copernicus Land Monitoring Service, geoportal: https://land.copernicus.eu/pan-european/corine-land-cover/clc-2012

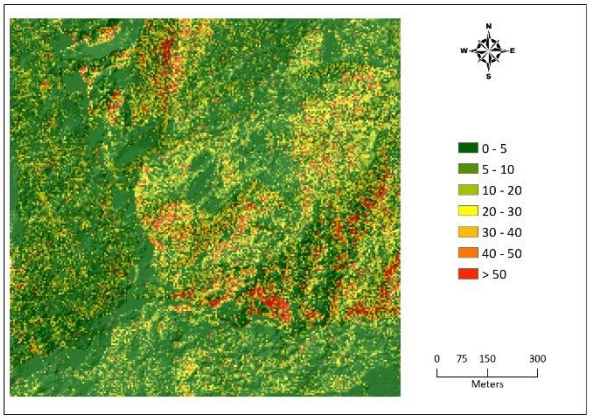

(Map 1a)

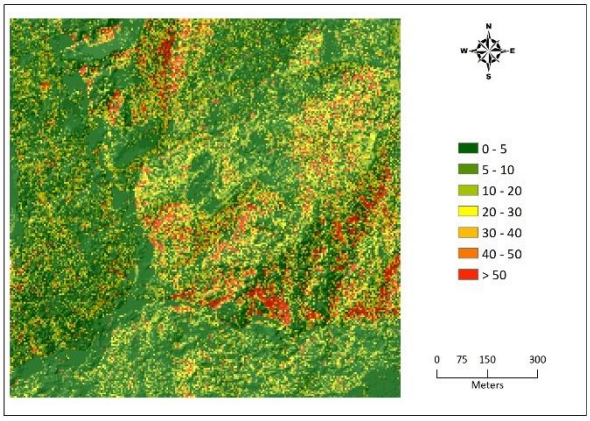

(Map 1b)

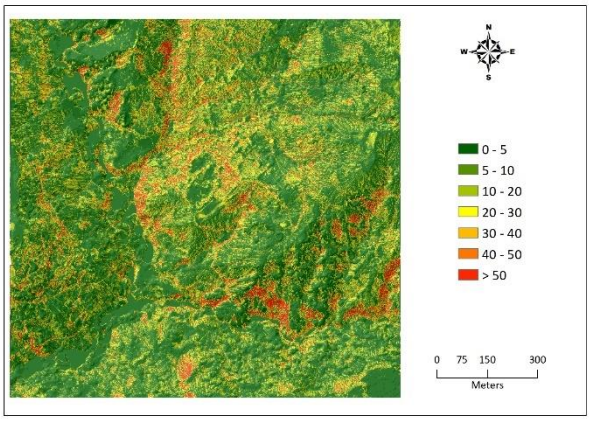

(Map 2a)

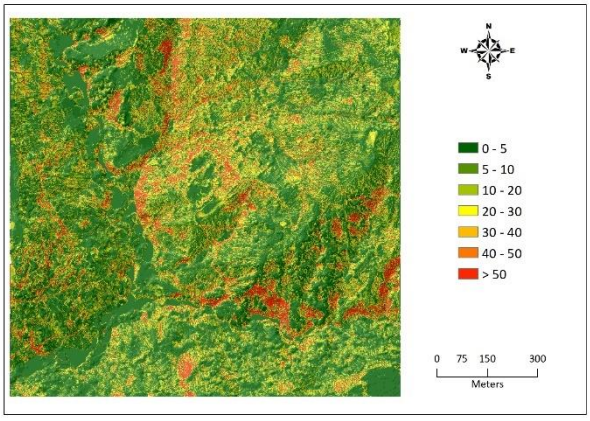

(Map 2b)

Figure 3. Soil loss rate (t ha^{-1} $year^{-1}$) estimation. The maps produced correspond to the four alternatives of Table 4.

D. *Results*

The study area's soil loss (t ha^{-1} $year^{-1}$) is estimated for the two land cover classification schemes under the 2011-2013 (present) RCP4.5 and the 2031-2050 (future) RCP8.5 scenarios. Table 4 summarizes the four estimated alternatives. These alternatives were selected in order to showcase the effect of climate change in its extreme occurrence, under land covers from existing databases (CLC 2012) or from classified UAV multispectral imagery.

Table 4. Numbering of the four estimated alternatives

	Land Cover Classification Scheme	
Scenario	CLC 2012	UAV classification
2011-30 RCP4.5	1a	2a
2031-50 RCP8.5	1b	2b

The spatial distribution of soil loss rate per case (Maps 1a, 1b, 2a, 2b) is depicted in Figure 3, while the percentage of area affected per case and per soil loss rate class (from very low to very high, or from 0 to > 50 t ha^{-1} $year^{-1}$) is presented in Table 5. In all cases, upper parts of the landscape with more steep slopes display the highest rates.

Table 5. Soil Loss classes by area (%) affected

	Area affected (%)			
Soil loss rates	1a	1b	2a	2b
Very Low	52.11	47.63	50.05	45.80
Low	17.96	17.42	17.33	16.71
Moderately Low	14.95	16.41	15.63	16.60
Moderate	5.96	7.05	6.76	7.72
Moderately High	2.92	3.49	3.46	4.21
High	1.71	2.12	1.99	2.50
Very High	4.39	5.88	4.78	6.46

The classification scheme affects the spatial distributions, with a greater percentage (of) area befalling under classes of higher rates in cases 2a/ 2b compared to cases 1a/ 1b. The same applies when future trends are considered: cases 1b/ 2b compared to 1a/ 2a. Overall, over 7 % of the total area 'moves' from the two lower soil loss classes (very low, low) to the rest of the classes, under the combined influence of future rainfall erosivity and UAV image classification land cover scheme.

III. Conclusions

In this paper, the soil loss by water erosion was estimated in the mountainous region of Metsovo. Towards this end, refined and adjusted input data from the UAV captures were utilized, enhancing the quality of the C-, LS-, and P- factors, while R-factor was parameterized based on present and future RCP scenarios from downscaled climatic models. The multifarious input data were processed, analyzed, and integrated into a GIS-based methodology. In this sense, this research study provides a methodology for both calculating soil loss by using refined data for the present conditions, and estimating future soil loss based on

potential changes of rainfall erosivity under different land cover classification schemes.

Land cover classification influences soil loss rates: the enhanced values of the P-factor derived from UAV's collected data yield higher soil loss values, and larger areas are ranked as more susceptible to water erosion. Existing land cover maps lead to the underestimation of soil loss rates of the area, while the systematic and adjusted image capturing, along with ground truthing, leads to the optimization of the generated land cover and soil loss maps.

Changes due to the climate change-based rainfall erosivity are expected to 'push' areas of lower erosion rate classes towards much higher ones. Since these higher erosion classes are going to be 'displaced', mainly towards the upper convex hillslope landscape parts, serious concerns are raised regarding terrain deformation, land(scape) degradation and productivity loss. Support and other management practices need to be considered, if the Metsovo region is to preserve its landscape form and agricultural productive base.

IV. Acknowledgements

This paper has been accomplished within the Research Project "Development of a system for monitoring and preventing natural disasters towards the climate change adaptation of Metsovo Municipality", under the aegis of EU and the National Strategic Reference Framework (NSRF) 2014-2020.

The authors acknowledge the E-OBS dataset from the EU-FP6 project ENSEMBLES (http://ensembles-eu.metoffice.com), the data providers in the ECA&D project (https://www.ecad.eu), the "Hydroscope" service for providing access to their data, the World Climate Research Programme's Working Group on Regional Climate, and the Working Group on Coupled Modelling, former coordinating body of CORDEX and responsible panel for CMIP5, the Earth System Grid Federation infrastructure, an international effort led by the U.S. Department of Energy's Program for Climate Model Diagnosis and Intercomparison, the European Network for Earth System Modelling and other partners in the Global Organisation for Earth System Science Portals (GO-ESSP). They also thank the KNMI and EC-EARTH modelling groups for producing and making available their model outputs.

References

Alexandridis, T.K., A.M. Sotiropoulou, G. Bilas, N. Karapetsas, N.G. Silleos (2015). The effects of seasonality in estimating the C-factor of soil erosion studies. *Land Degradation & Development*, Vol. 26(6), pp. 596-603.

Bangash, R.F., A. Passuello, M. Sanchez-Canales, M. Terrado, A. López, F.J. Elorza, ..., M. Schuhmacher (2013). Ecosystem services in Mediterranean river basin: climate change impact on water provisioning and erosion control. *Science of the Total Environment*, Vol. 458, pp. 246-255.

Casanueva, A, S. Kotlarski, S. Herrera, J. Fernández, J.M. Gutiérrez, …, R. Vautard (2015). Daily precipitation statistics in a EURO-CORDEX RCM ensemble: Added value of raw and bias-corrected high-resolution simulations. *Climate Dynamics*, Vol. 47, No. 3-4.

Dieckmann, H., H. Motzer, H.P. Harres, O. Seuffert (1992). Vegetation and erosion. Investigations on erosion plots in southern Sardinia. *Geo-Ö ko-Plus*. Vol. 3, pp. 139-149.

Diodato, N., and G. Bellocchi (2010). MedREM, a rainfall erosivity model for the Mediterranean region. *Journal of Hydrology*, Vol. 387, No. 1-2.

Flambouris, K. (2008). Study of rainfall factor on the RUSLE law. *Doctoral Thesis*, Aristotle University of Thessaloniki.

Flato, G., Marotzke, J., Abiodun, B., Braconnot, P., Chou, S. C., Collins, W., ... & Forest, C. (2013). Evaluation of climate models. In: *Climate Change 2013: The Physical Science Basis. Contribution of Working Group I to the Fifth Assessment Report of the Intergovernmental Panel on Climate Change*. Stocker T.F., Qin D., Plattner G.-K., Tignor M., Allen S.K., Doschung J., Nauels A., Xia Y., Bex V., Midgley P.M. (eds), Cambridge University Press, pp. 741-882.

Gupta, S., and S. Kumar (2017). Simulating climate change impact on soil erosion using RUSLE model – A case study in a watershed of mid-Himalayan landscape. *Journal of Earth System Science,* Vol. 126(3), pp. 43.

Hernando, D., and M. Romana (2015). Estimating the rainfall erosivity factor from monthly precipitation data in the Madrid Region (Spain). *Journal of Hydrology and Hydromechanics*, Vol. 63, No. 1.

Inbar, M., M.I. Tamir, and L. Wittenberg (1998). Runoff and erosion processes after a forest fire in Mount Carmel, a Mediterranean area. *Geomorphology*, Vol. 24 (1), pp. 17-33.

Jacob, D., J. Petersen, B. Eggert, A. Alias, O.B. Christensen, …, P. Yiou (2014). EURO-CORDEX: New high-resolution climate change projections for European impact research. *Regional Environmental Change*, Vol. 14, No. 2.

Julien, P.Y. (2010). Erosion and sedimentation. Cambridge University Press, UK.

Karydas, C.G., P. Panagos, and I.Z. Gitas (2014). A classification of water erosion models according to their geospatial characteristics. *International Journal of Digital Earth*, Vol. *7*(3), pp. 229-250.

Kosmas, C., N. Danalatos, D. Kosma, P. Kosmopoulou (2006). In: *Soil erosion in Europe*. Boardman J., Poesen J. (eds.), John Wiley & Sons, Chichester, pp. 279-288.

Lal, R. (2014). Desertification and soil erosion. In: *Global Environmental Change*, Springer, Dordrecht, pp. 369-378.

Li, Z., and H. Fang (2016). Impacts of climate change on water erosion: A review. *Earth-Science Reviews*, Vol. 163, pp. 94-117.

Maeda, E.E., P.K. Pellikka, M. Siljander, B.J. Clark (2010). Potential impacts of agricultural expansion and climate change on soil erosion in the Eastern Arc Mountains of Kenya. *Geomorphology*, Vol. 123 (3-4), pp. 279-289.

McNabb, D.H., and F.J. Swanson (1990). Effects of fire on soil erosion. In: *Natural and Prescribed Fire in Pacific Northwest Forests*. Walstad J.D, Radosevich S.R., Sandberg D.V. (eds.), Oregon State Univ. Press, Corvallis, Oregon, pp. 159–173.

Mearns, L.O., S.H. Schneider, S.L. Thompson, L.R. McDaniel (1989). Climate variability statistics from general circulation

models as applied to climate change analysis. In: *Natural areas facing climate change.* Malanson G.P. (ed.), SPB Academic Publishing, The Hague, 5173.

Moore, I.D., and G.J. Burch (1986a). Physical Basis of the Length-slope Factor in the Universal Soil Loss Equation. *Soil Science Society of America Journal*, Vol. 50 (5), pp. 1294-1298.

Moore, I.D., and G.J. Burch (1986b). Modelling erosion and deposition: topographic effects. *Transactions of the ASAE*, Vol. 29(6), pp. 1624-1630.

Morgan, R.P.C., and M. Nearing (2011). *Handbook of Erosion Modelling*. John Wiley & Sons, New York.

Mullan, D., D. Favis-Mortlock, and R. Fealy (2012). Addressing key limitations associated with modelling soil erosion under the impacts of future climate change. *Agricultural and Forest Meteorology,* Vol. 156, pp. 18-30.

Nearing, M.A., Y. Xie, B. Liu, Y. Ye (2017). Natural and anthropogenic rates of soil erosion. *International Soil and Water Conservation Research*, Vol. 5(2), pp. 77-84.

Nearing, M.A., F.F. Pruski, and M.R. O'neal (2004). Expected climate change impacts on soil erosion rates: a review. *Journal of soil and water conservation*, Vol. 59 (1), pp. 43-50.

Nunes, J.P., and M.A. Nearing (2010). Modelling impacts of climatic change: case studies using the new generation of erosion models. *Handbook of Erosion Modelling*, pp. 289-312.

Panagos, P. (2006). The European soil database. *GEO: connexion*, Vol. 5(7), pp. 32-33.

Panagos, P., K. Meusburger, C. Ballabio, P. Borrelli, C. Alewell (2014). Soil erodibility in Europe: a high-resolution dataset based on LUCAS. *Science of the total environment*, Vol. 479, pp. 189-200.

Panagos, P., P. Borrelli, J. Poesen, C. Ballabio, E. Lugato, K. Meusburger, ..., C. Alewell (2015a). The new assessment of soil loss by water erosion in Europe. *Environmental science & policy*, Vol. 54, pp. 438-447.

Panagos, P., P. Borrelli, K. Meusburger, C. Alewell, E. Lugato, L. Montanarella (2015b). Estimating the soil erosion cover-management factor at the European scale. *Land use policy*, Vol. 48, pp. 38-50.

Panagos, P., C. Ballabio, K. Meusburger, J. Spinoni, C. Alewell, P. Borrelli (2017). Towards estimates of future rainfall erosivity in Europe based on REDES and WorldClim datasets. *Journal of Hydrology*, Vol. 548.

Panagos, P., C. Ballabio, P. Borrelli, K. Meusburger (2016). Spatio-temporal analysis of rainfall erosivity and erosivity density in Greece. *Catena*, Vol. 137.

Panagos, P., C. Ballabio, P. Borrelli, K. Meusburger, A. Klik, S. Rousseva, M.P. Tadić, S. Michaelide, M. Hrabalíková, P. Olsen, J. Aalto, M. Lakatos, A. Rymszewicz, A. Dumitrescu, S. Beguería, C. Alewell (2015c). Rainfall erosivity in Europe. *Science of The Total Environment*, Vol. 511, No. 1.

Parajuli, P.B., P. Jayakody, G.F. Sassenrath, Y. Ouyang (2016). Assessing the impacts of climate change and tillage practices on stream flow, crop and sediment yields from the Mississippi River Basin. *Agricultural Water Management*, Vol. 168, pp. 112-124.

Pepin N, R.S. Bradley, H.F. Diaz, M. Baraer, E.B. Caceres, N. Forsythe, H. Fowler, G. Greenwood, M.Z. Hashmi, X.D. Liu, J.R. Miller, L. Ning, A. Ohmura, E. Palazzi, I. Rangwala, W. Schöner, I. Severskiy, M. Shahgedanova, M.B. Wang, S.N. Williamson, D.Q. Yang (2015). Elevation-dependent warming in mountain regions of the world. *Nature Climate Change*, Vol. 5, No. 5.

Pimentel, D. (2006). Soil erosion: a food and environmental threat. *Environment, development and sustainability*, Vol. 8(1), pp. 119-137.

Prasannakumar, V., H. Vijith, S. Abinod, N. Geetha (2012). Estimation of soil erosion risk within a small mountainous sub-watershed in Kerala, India, using Revised Universal Soil Loss Equation (RUSLE) and geo-information technology. *Geoscience Frontiers*, Vol. 3(2), pp. 209-215.

Pruski, F.F., and M.A. Nearing (2002). Climate-induced changes in erosion during the 21st century for eight US locations. *Water Resources Research*, Vol. 38(12).

Renard, K.G., G.R. Foster, G.A. Weesies, D.K. McCool, D.C. Yoder (1997). Predicting Soil Erosion by Water: A Guide to Conservation Planning with the Revised Universal Soil Loss Equation (RUSLE). *Agricultural Handbook 703,* US Department of Agriculture, Washington, DC.

Sakellariou, A., D. Koutsoyiannis, and D. Tolikas (1994). HYDROSCOPE: Experience from a Distributed Database System for Hydrometeorological Data. In: *International Conference on Hydraulic Engineering Software*, Hydrosoft, Proceedings, Vol. 2, pp. 309–316.

Shi, Z.H., C.F. Cai, S.W. Ding, T.W. Wang, T.L. Chow (2004). Soil conservation planning at the small watershed level using RUSLE with GIS: a case study in the Three Gorge Area of China. *Catena*, Vol. 55(1), pp. 33-48.

Shiono, T., S. Ogawa, T. Miyamoto, K. Kameyama (2013). Expected impacts of climate change on rainfall erosivity of farmlands in Japan. *Ecological Engineering,* Vol. 61 (Part C).

Solomon, A.M., and R. Leemans (1997). Boreal forest carbon stocks and wood supply: past, present and future responses to changing climate, agriculture and species availability. *Agricultural and Forest Meteorology*, Vol. 84 (1-2), pp. 137-151.

Van der Knijff, J.M.F., R.J.A. Jones, and L. Montanarella (1999). *Soil erosion risk assessment in Italy*. European Soil Bureau, European Commission.

Van Liedekerke, M., A. Jones, and P. Panagos (2006). ESDBv2 Raster Library-a set of rasters derived from the European Soil Database distribution v2.0. *European Commission and the European Soil Bureau Network,* CDROM, EUR, 19945.

Wainwright, J., A.J. Parsons, K. Michaelides, D.M. Powell, R. Brazier (2003). Linking Short-and Long-Term Soil—Erosion Modelling. In: *Long Term Hillslope and Fluvial System Modelling*. Lang A., Hennrich K., Dikau R. (eds.), Lecture Notes in Earth Sciences. Springer-Verlag, Berlin, Heidelberg, pp. 37-51.

Yang, X., X. Xie, D.L. Liu, F. Ji, L. Wang (2015). Spatial Interpolation of Daily Rainfall Data for Local Climate Impact Assessment over Greater Sydney Region. *Advances in Meteorology*, Vol. 2015.

Yin, S., Y. Xie, B. Liu, M.A. Nearing (2015). Rainfall erosivity estimation based on rainfall data collected over a range of temporal resolutions. *Hydrology and Earth System Sciences*, Vol. 19, No. 10.

Zhang, X.C.J. (2012). Cropping and tillage systems effects on soil erosion under climate change in Oklahoma. *Soil Science Society of America Journal*, Vol. 76 (5), pp. 1789-1797.